

# Induced Compton Scattering in Gigahertz Peak Spectrum Radio Sources

Zdenka Kuncic<sup>1</sup>, Geoffrey V. Bicknell

Astrophysical Theory Centre<sup>2</sup>,  
Australian National University, Canberra, ACT 0200, Australia

and

Michael A. Dopita

Mount Stromlo and Siding Spring Observatories, Weston PO, ACT 2611, Australia

## ABSTRACT

We revisit the shocked shell model for the class of Active Galactic Nuclei known as Gigahertz Peak Spectrum sources, incorporating new observational data on the radiation brightness temperatures. We argue that in addition to free-free absorption, induced Compton scattering will also have an important effect in forming the  $\sim$  GHz peak and in shaping the radio spectra that characterize these sources. Indeed, our arguments suggest that GPS sources may provide the first real evidence for the role of induced Compton scattering in extragalactic radio sources.

*Subject headings:* galaxies: active — shocks — radiation mechanisms: thermal, non-thermal — scattering

## 1. Introduction

Recently, Bicknell, Dopita, & O’Dea (1997) developed a model which unifies the Gigahertz Peak Spectrum (GPS) sources and the related Active Galactic Nuclei (AGN) classes known as Compact Steep Spectrum (CSS) sources and Compact Symmetric Objects

---

<sup>1</sup>Now at Dept. Physics & Astronomy, University of Victoria, B.C., V8W 3P6, Canada. Email: zdenka@uvastro.phys.uvic.ca.

<sup>2</sup>The ANUATC is jointly operated by the Mount Stromlo and Siding Spring Observatories and the School of Mathematical Sciences.

(CSOs). Their model attributes the observed radio spectra and optical emission to the interaction of a jet–driven, non–thermal lobe with the ambient galactic interstellar medium (ISM). As the radio lobe forces its way through the ISM, strong radiative shocks create shells of shock–ionized and photo–ionized gas which produce a low–frequency break in the power law spectrum through free–free absorption (FFA). Although synchrotron self–absorption (SSA) provides a natural mechanism to produce a low frequency break in a non–thermal spectrum and is successful in explaining the spectra of AGN with distinct core–jet morphologies (Blandford & Königl 1979), we expect that it is unimportant in the more extended jet lobes of GPS sources, where the non–thermal plasma is more likely to be optically–thin to its own radiation. However, the spectrum emitted by the non–thermal lobe plasma can still exhibit a low frequency break not only as a result of FFA in an external shell of thermal gas surrounding the lobe, as suggested by Bicknell et al. (1997), but also as a result of the competing low–frequency process of induced Compton scattering (ICS).

ICS becomes important in a high brightness temperature radiation field, such as that which is readily generated by synchrotron radio sources and which has a Thomson scattering optical depth  $\tau_T$  and a brightness temperature  $kT_{b,\nu} \gg m_e c^2 \gg h\nu$ , such that

$$\left(f \frac{kT_{b,\nu}}{m_e c^2}\right) \tau_T \gtrsim 1, \quad (1)$$

where the parameter  $f$  quantifies the strong effect of the angular distribution of the radiation and is given by:

$$f \approx \frac{3}{16\pi} \int (1 + \cos^2 \phi)(1 - \cos \phi) d\Omega \quad (2)$$

where  $\phi$  is the scattering angle and the integral is over the solid angle of the beam incident on the scattering region (Coppi, Blandford & Rees 1993). For a conical beam of radiation with half angle  $\cos^{-1}(\mu_0)$  and solid angle  $\Omega_0$ ,  $f = (1 - \mu_0)^2(3\mu_0^2 + 2\mu_0 + 7)/32$ ; for complete isotropy of the radiation field  $f = 1$ ; for  $\mu_0$  near unity,  $f \approx \frac{3}{8}(1 - \mu_0)^2$ . In both cases  $f \approx (\Omega_0/4\pi)^2$ . ICS redistributes photon energies from frequencies near where  $T_{b,\nu}$  peaks to lower frequencies where they are absorbed (e.g. by SSA or FFA) effectively reducing the peak  $T_{b,\nu}$  observed. As first demonstrated by Sunyaev (1970), the key observational consequence is a break in synchrotron radio spectra.

Equation (1) implies that induced scattering can produce spectral distortions when  $\tau_T \gtrsim (5 \times 10^9)K/fT_b$  and hence, unlike ‘ordinary’ (spontaneous) Compton scattering, it can be important even when  $\tau_T < 1$ . Indeed, for a typical synchrotron radio source, ICS can be more efficient than SSA in producing a spectral turnover and can limit the brightness temperature at GHz frequencies to  $T_{b,1\text{GHz}} \lesssim 10^{11} \nu_9^{-0.2} \gamma_{\text{min}}^{0.6}$  K, where  $\gamma_{\text{min}}$  is the

low-energy cutoff to the non-thermal electron distribution<sup>3</sup> (Sincell & Krolik 1994). Note that this limit is only weakly dependent on the source parameters and (for  $f \sim 1$ ) is lower than the theoretical inverse Compton limit,  $T_b \lesssim 10^{12}$  K, for typical AGN sources (Hoyle, Burbidge & Sargent 1966). As argued by Sincell & Krolik (1994), ICS may explain why the inverse Compton limit is, in practice, rarely observed. Such is the case for GPS sources, where the observed brightness temperatures of lobe subcomponents are typically  $10^{9-10}$  K (Stanghellini et al. 1997). Since ICS by the non-thermal, relativistic electrons in the jet lobes cannot reduce the intrinsic peak  $T_b$  to these observed levels, then ICS may instead be operating externally. Indeed, Coppi, Blandford & Rees (1993) have shown that ICS by relatively ‘cold’ (nonrelativistic) electrons outside of a primary non-thermal source can effectively reduce the peak brightness temperature to values such that  $kT_b \simeq m_e c^2$  and this alone makes it very tempting to adopt such a scenario to explain the observed  $T_b$  values in GPS sources.

In this *Letter*, we examine the process of induced scattering to show that in order to account for the observed brightness temperatures in GPS sources, this process must be operating at some level in the shock-ionized shell that has been postulated to surround the non-thermal lobes.

## 2. The Case for Induced Scattering in GPS Sources

In the scenario proposed by Bicknell et al. (1997), the non-thermal jet lobes in GPS sources are surrounded by a shell of thermal, nonrelativistic plasma formed from shocked and photoionized material in the ambient ISM. Although FFA is likely to be operating at some level in this external shell, there will be strong competition from ICS, especially if the shell is tenuous. Indeed, with the expected brightness temperatures,  $\sim 10^{11}$  K, of the primary non-thermal radiation which impinges upon the shell, ICS is more efficient than FFA in producing a break at  $\sim$  GHz frequencies when the electron number density,  $n_e$ , satisfies

$$n_e \ll 100 \nu_9^2 T_4^{3/2} \left( \frac{T_{b,1\text{GHz}}}{10^{11}\text{K}} \right) \text{ cm}^{-3}, \quad (3)$$

where the electron temperature,  $T_e = 10^4 T_4$  K. This is precisely the range of densities relevant to shock-ionized ISM material surrounding jet lobes in GPS sources, as found by Bicknell et al. (1997). Although, in general, collective plasma effects will not have an

---

<sup>3</sup>A characteristic power-law index of 2.4 has been assumed here for the electron distribution. According to standard synchrotron theory, this corresponds to a spectral index of  $\alpha \simeq 0.7$ , which is a fiducial value for the GPS sources we are concerned with here (Bicknell et al. 1997).

overall affect on ICS (see Coppi, Blandford & Rees 1993), this is not strictly the case in the presence of a high brightness temperature radiation field, which can trigger stimulated Raman scattering, whereby the radio waves scatter off plasmons (Langmuir waves) rather than off the individual electrons themselves. Since, at the densities relevant here, this process requires brightness temperatures  $\gtrsim 10^{14}$  K (Levinson & Blandford 1995), it is unlikely to be important in this context.

A definitive test for any model which attempts to explain the spectral peak in GPS/CSS sources is the observed inverse correlation between the frequency at which the spectrum peaks,  $\nu_p$ , and the source size. In the FFA model of Bicknell et al. (1997), a theoretical relationship between these two parameters readily emerges from the shock dynamics. We follow the same method here in constructing an analogous ICS model, but as we explain below, the predicted relationship has different dependences on the physical parameters.

A spectral break due to ICS is expected at the frequency where the optical depth, given by the left hand side of equation (1), reaches unity. However, as equations (1) and (2) show, induced scattering depends strongly on the angular distribution of the high brightness temperature radiation field and we have allowed for this through the parameter  $f$ . The flux density corresponding to the condition on the brightness temperature is obtained by simply integrating the surface brightness over the solid angle  $\Omega$  subtended by the source at the observer, giving

$$\nu^{-2} F_\nu = 2m_e \int (f \tau_T)^{-1} d\Omega. \quad (4)$$

In the model developed by Bicknell et al. (1997),  $\tau_T$  is approximately uniform over the sides of the lobe and the solid angle can be expressed as  $\Delta\Omega \simeq \pi r_c x_h / D^2 = \pi \zeta^{-1/2} x_h^2 / D^2$ , where  $r_c$  is the radius of the semi-ellipsoidal cocoon which forms as the jet-driven lobe expands into the ISM,  $x_h$  is the distance from the core at the base of the jet to the lobe hotspot (i.e. the semi-major axis of the cocoon),  $D$  is the distance to the source and  $\zeta (\simeq 2$  typically) is the ratio of the averaged hotspot pressure to cocoon pressure. By taking a power-law spectrum,  $F_\nu = F_{\nu_0} (\nu/\nu_0)^{-\alpha}$ , where  $\nu_0$  is a fiducial frequency (5 GHz in this case), and using the monochromatic power  $P_{\nu_0} = 4\pi D^2 F_{\nu_0}$ , equation (4) predicts a peak frequency given by

$$\frac{\nu_p}{\nu_0} \simeq \left[ \frac{f \zeta^{1/2} P_{\nu_0} \tau_T}{8\pi^2 x_h^2 \nu_0^2 m_e} \right]^{\frac{1}{\alpha+2}}, \quad (5)$$

where  $P_{\nu_0} = 4\pi D^2 F_{\nu_0}$  is the monochromatic power.

The Thomson optical depth is assumed to be approximately uniform over the sides of the lobe and is calculated with the MAPPINGSII code (Sutherland & Dopita 1993) for radiative shocks, giving

$$\tau_T \simeq (4.9 \times 10^{-3}) V_3^{3.6} + (1.6 \times 10^{-2}) V_3^{2.5}, \quad (6)$$

where  $V = 1000V_3 \text{ km s}^{-1}$  is the shock velocity corresponding to the sideways expansion of the radio lobe. The two terms correspond to the shocked gas and photoionized precursor. Specifically, the shock velocity is given by (see equations 2-10 and 2-11 in Bicknell et al. 1997)

$$V_3 = V_{0,3} \left( \frac{x_h}{\text{kpc}} \right)^{\frac{\delta-2}{3}}, \quad (7)$$

where

$$V_{0,3} = 1.5 \left( \frac{6}{8-\delta} \right)^{1/3} \zeta^{1/6} \left[ \frac{F_{E,45}}{n_0} \right]^{1/3} \quad (8)$$

and where  $F_E = 10^{45} F_{E,45} \text{ erg s}^{-1}$  is the jet energy flux and  $\delta$  is the power-law index of the Hydrogen density distribution, given by  $n_H = n_0 (x_h/\text{kpc})^{-\delta}$ .

Equation (5) predicts a relationship between peak frequency and source size that derives quite differently from that predicted by the FFA model (see equation 5-10 in Bicknell et al. (1997)). Since the opacity of ICS is proportional to the radiation brightness temperature, the chief dependence of  $\nu_p$  derives from the integrated surface brightness ( $\propto x_h^2$ ). There is also a weaker dependence on  $x_h$  through the shock velocity, as given in equation (7), which in turn determines  $\tau_T$ . In the case of the FFA model, on the other hand, while there is also a similar weak dependence through  $V$ , the predicted  $\nu_p - x_h$  relationship derives chiefly from the dependence on density (which has a power-law scaling with source size). This density dependence arises simply because the opacity due to FFA is  $\propto \int n_e^2 dl$ , whereas for ICS, it is  $\propto \int n_e dl$  where both integrals are through the ionized screen. Allowing for the inverse dependence of the shocked cooling zone and the photoionized precursor on density, the dependences on density are respectively on the first and zeroth powers of  $n_e$ . This is reflected, for instance, in the dependence of the Thomson optical depth on velocity alone and this is where a dependence on density does enter, since the expansion velocity is a function of the ambient density. Although these two different models predict a  $\nu_p - x_h$  relationship that derives from intrinsically different physical processes (i.e. two-body interactions versus particle-photon interactions), the overall differences are surprisingly small: both FFA and ICS models predict a negative slope in the  $\nu_p - x_h$  plane which is close to unity and which varies very weakly with the relevant range of parameters.

Let us now examine the predicted peak frequency - source size relationship more quantitatively.

### 3. Results

The relationship between peak frequency,  $\nu_p$ , and source size,  $x_h$ , as predicted by equation (5) for the anisotropy parameter  $f = 1$  is plotted and compared with observational data (Fanti et al. 1990, Stanghellini et al. 1997, O’Dea & Baum 1997) in figure 1. The parameters involved in the theoretical lines are as follows: values of the Hydrogen densities at 1 kpc,  $n_0$ , are 1 and  $10\text{ cm}^{-3}$ ; values of the density power-law index,  $\delta$ , are 1.5 and 2 (these are the lower and upper limits suggested by Begelman (1996) in his fit to the luminosity-size relation for CSOs); the total 5 GHz radio power is  $P_{5\text{GHz}} = 10^{27.5}\text{ erg s}^{-1}\text{ Hz}^{-1}$ , corresponding to the average radio power of GPS sources (Fanti et al. 1990, Stanghellini et al. 1997); the jet energy flux is  $F_E = 10^{45}\text{ ergs s}^{-1}$  and the spectral index is  $\alpha = 0.7$  (Bicknell et al. 1997). Table 1 lists the values of the parameter  $V_{0,3}$ , which provides the scale for the size of the velocity as a function of source size (see eq. [8]).

The slopes of both the  $\delta = 1.5$  and  $\delta = 2$  lines are adequate fits to the slope of the data points and the overall fits to the data are obviously better for the lower values of  $n_0$ . The fits could also be improved by increasing the radio power and Thomson optical depth. Increasing the radio power increases the brightness temperature of the lobe and hence the frequency at which induced Compton scattering becomes important. We have not decreased the density still further to produce a more acceptable fit since it is evident from table 1 that lower densities would involve an unacceptable extrapolation of the fit to the Thomson opacity, well beyond the velocities of  $\sim 1000\text{ km s}^{-1}$  that the MAPPINGSII code can adequately handle. Indeed, the velocity in even the  $\delta = 1.5$ ,  $n_0 = 10$  model is greater than  $1000\text{ km s}^{-1}$  for an overall size  $\lesssim 0.5\text{ kpc}$ . It can be reasonably assumed, however, that the lower densities favoured by our ICS model imply cocoon velocities in excess of  $1000\text{ km s}^{-1}$ , even if the extrapolation of the shock modeling beyond such a velocity is uncertain.

### 4. Discussion

Our model assumes a uniform distribution of radio emitting plasma in the jet lobes, whereas in a number of imaged GPS sources, the emitting region is clumpy; the highest brightness temperatures are typically identified with a small number of localized components (Stanghellini et al. 1997, Conway et al. 1994, Wikinson et al., 1994). If these clumps were embedded in a lower surface brightness cocoon outside of which the ionizing screen were located then the radiation intercepting this screen would be anisotropic. This effect of anisotropy is countered however, by the power (typically  $1/2.7$ ) entering in the expression for  $\nu_p$ . Thus,  $\nu_p$  would be reduced to approximately 40% of the isotropic value for  $f \sim 0.1$ . Moreover, as inspection of the images of GPS and CSO sources (the latter all being GPS)

reveals, the "clumps" are usually situated at increasing distances from the nucleus with a local filling factor of order unity. The beam solid angle corresponding to each clump should therefore be of order  $2\pi$ . Anisotropy need not be an important factor especially in view of the insensitivity of the peak frequency to it.

On the other hand, non-uniformity in the emission increases the brightness temperature. In our uniform model, the brightness Temperature at 5 GHz, is given by:

$$\langle T_{b,5\text{GHz}} \rangle \simeq \frac{\zeta^{1/2} c^2 P_\nu}{8\pi^2 x_p^2 \nu^2 k} \simeq 10^{10} \left( \frac{P_{5\text{GHz}}}{10^{27.5} \text{ W Hz}^{-1}} \right) \left( \frac{x_h}{100\text{pc}} \right)^{-2} \left( \frac{\nu}{5 \times 10^9 \text{ Hz}} \right)^{-2} \text{ K}. \quad (9)$$

and is about an order of magnitude lower than the values observed in subcomponents by Stanghellini et al. 1997, for example. A larger brightness temperature of course *enhances* the prospect of induced Compton scattering.

Interestingly, the Stanghellini et al. study of a complete sample of GPS sources has revealed a pronounced peak in the distribution of low-frequency spectral indices near  $\alpha = -1.0$ , which is in remarkable agreement with the theoretically predicted spectra resulting from induced Compton scattering by external thermal electrons (e.g. Coppi, Blandford & Rees 1993). This feature, combined with the successful ICS explanation for the peak frequency – source size relationship, shows that GPS sources may indeed constitute the first real instance where induced Compton scattering plays a relatively clear role in extragalactic radio sources.

We therefore conclude that induced Compton scattering may be an important process in the shocked and photoionized plasma surrounding an expanding lobe in GPS sources; it can contribute to the formation of the characteristic peak in the radio spectrum when the density falls below  $\sim 10 \text{ cm}^{-3}$  and free-free absorption becomes inefficient. Expansion velocities of  $1000 - 2000 \text{ km s}^{-1}$  are then implied when induced scattering is the dominant process. Induced scattering may thus be particularly relevant in the high redshift GPS sources (Elvis et al. 1997), which have column depths of the order of a few  $\times 10^{22} \text{ cm}^{-2}$ , at the lower end of the range estimated by Bicknell et al. (1997) on the basis of the FFA model.

In general, the introduction of induced Compton scattering not only increases the range of plasma densities over which a low frequency break can be produced, but also increases the efficiency of FFA at the lowest frequencies, where photons are being continuously replenished as a result of the downscattering of GHz photons. Indeed, the combined effect of induced scattering and free-free absorption could also be important in some other sources, such as NGC 1275, in which one of the jets appears to be significantly weaker than the other at low frequencies. This has been attributed to free-free absorption (Levinson, Laor

& Vermeulen 1995) and although the observations are on parsec scales in this particular source, the brightness temperatures are similar to the values considered here, suggesting that induced Compton scattering may well be operating on various jet scales, at the very least in conjunction with the more conventional process of free–free absorption.

We wish to thank Professor Rashid Sunyaev for suggesting that we consider ICS for GPS sources and our anonymous referee whose valuable comments and suggestions helped to improve the paper significantly. We also thank Chris O’Dea for helpful comments.

### REFERENCES

- Begelman, M. C. 1996, *Cygnus A: Study of a Radio Galaxy* (Cambridge: CUP), 209
- Bicknell, G. V., Dopita, M. A., & O’Dea, C. P. 1997, preprint
- Blandford, R. D. & Königl, A. 1979, *ApJ*, 232, 34
- Conway J.E., Myers S.T., Pearson T.J., Readhead A.C.S., Unwin S.C. and Xu W., 1994, *ApJ*, 425, 568
- Coppi, P., Blandford, R. D., & Rees, M. J. 1993, *MNRAS*, 262, 603
- Elvis, M., Fiore, F., Giommi, P., & Padovani, P. 1997, *ApJL*, in press
- Fanti, R., Fanti, C., Schilizzi, R. T., Spencer, R. E., Rendong, N., Parma, P., Van–Breugel, W. J. M., & Venturi, T. 1990, *Astron. Astrophys.*, 231, 333
- Hoyle, F., Burbidge, G. R. & Sargent, W. L. W. 1966, *Nature*, 209, 751
- Levinson, A. & Blandford, R. D. 1995, *MNRAS*, 274, 717
- Levinson, A., Laor, A. & Vermeulen, R. C. 1995, *ApJ*, 448, 589
- O’Dea, C. P. & Baum, S. A. 1997, *Astron. Astrophys.*, submitted
- Sincell, M. W. & Krolik, J. H. 1994, *ApJ*, 430, 550
- Sincell, M. W. & Coppi, P. S. 1996, *ApJ*, 460, 163
- Stanghellini, C., O’Dea, C. P., Baum, S. A., & Fanti, R. 1997, in preparation
- Sunyaev, R. A. 1970, *Astrophys. Lett.*, 7, 19



Sutherland, R. A. & Dopita, M. A. 1993, ApJS, 88, 253

Wilkinson P.N., Polatidis A.G., Readhead A.C.S., Xu W. and Pearson T.J., 1994, ApJ, 432,  
L87

### Figure Caption

Fig. 1.— A comparison of the predicted and observed relationship between the peak frequency and source size for GPS sources. The lines represent the theoretical relationship predicted by equation (5): solid and dashed lines are for  $\delta = 2.0$  and  $\delta = 1.5$ , respectively (values of  $n_0 = 1 \text{ cm}^{-3}$  and  $n_0 = 10 \text{ cm}^{-3}$  are indicated) and the other values used are  $\alpha = 0.7$ ,  $P_{5\text{GHz}} = 10^{27.5} \text{ W Hz}^{-1}$  and  $F_E = 10^{45} \text{ erg s}^{-1}$  (see the text for definitions of these parameters). The data points are from Fanti et al. (1990), O’Dea & Baum (1997) and Stanghellini et al. (1997).

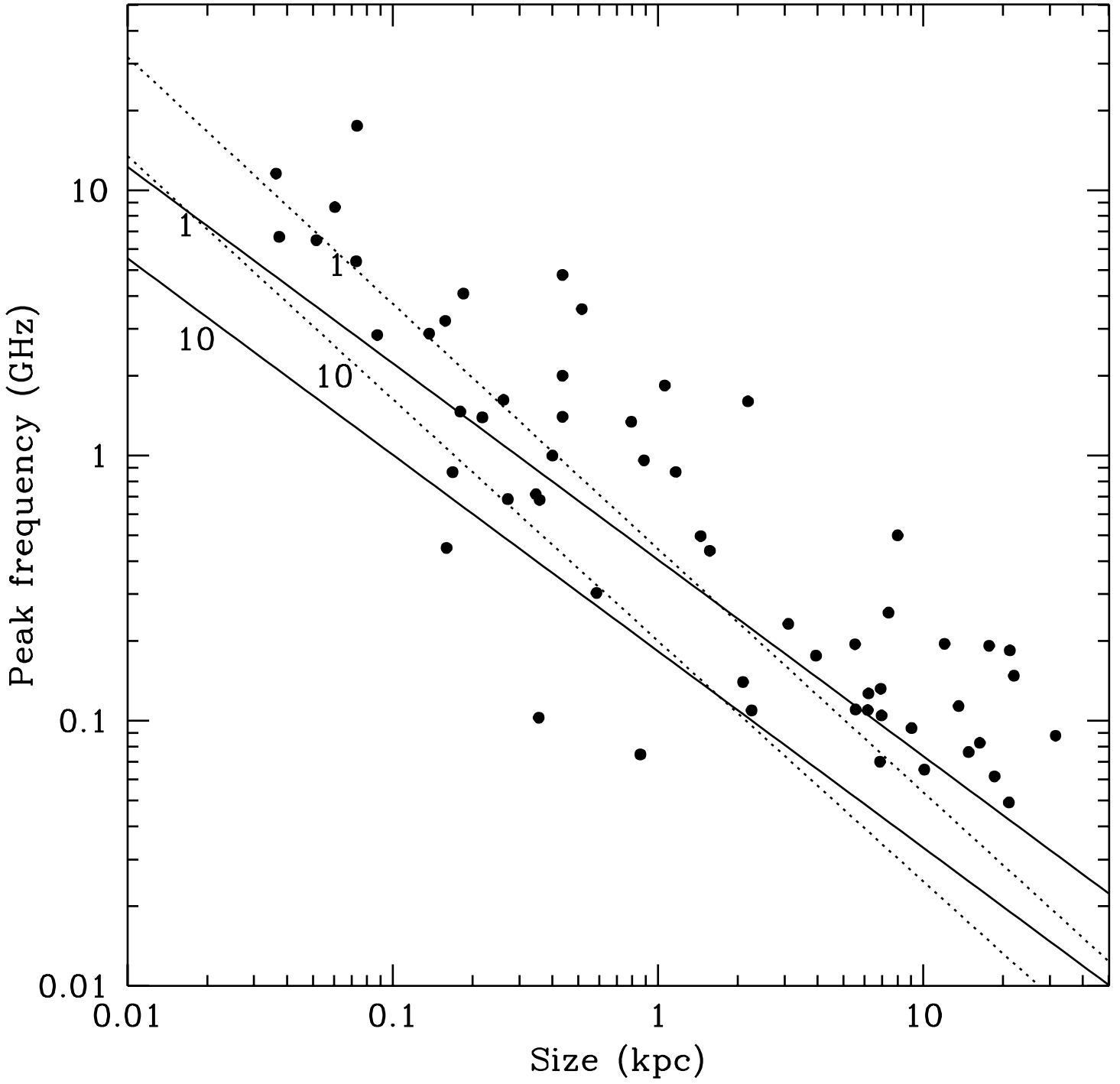


**Table 1: Parameters of expanding cocoon**

$n_0$ $\text{cm}^{-3}$	$\delta$	$V_{0,3}$
1	2	1.80
10	2	0.84
1	1.5	1.75
10	1.5	0.81